DOI: 10.1002/ejic.200500952

The First Example of a Dinuclear Platinum(III) Complex with Three Bridging Ligands

Raffaella Z. Pellicani,[a] Francesco P. Intini,[a] Luciana Maresca,[a] Ernesto Mesto,[b] Concetta Pacifico,[a] and Giovanni Natile*[a]

Keywords: Bridging ligands / Hydrogen bonds / Metal–metal interactions / N ligands / Platinum(III)

The first triply bridged dinuclear platinum(III) compound with acetamidate ligands, $X[Pt_2Cl_4\{N(H)C(CH_3)O\}_3]$ ($X = K^+$ or $AsPh_4^+$), has been isolated in the solid state and characterized by one- and two-dimensional NMR spectroscopy and X-ray crystallography. Owing to the asymmetry of the bridging acetamidate ligands, three isomers can be formed (HHH, HHT, and HTH), although only two are found in the crude reaction product: HHT and HTH. The HTH species is thermodynamically less stable and slowly (half life of around two days at room temperature) isomerizes into the HHT form. The more stable and less symmetric HHT isomer crystallizes from chloroform/pentane ($AsPh_4^+$ counter ion). The two $[Pt_2Cl_4\{N(H)C(CH_3)O\}_3]^-$ anions of the unit cell are linked by two strong N–H···O H-bonds while contiguous anions of adjacent cells are linked together by two, slightly weaker N–H···Cl H-bonds. The result is a chain of anions running along the *a* direction. The crystal packing allows for the formation of one-dimensional pore channels, also running along the *a* direction, which are filled with disordered pentane molecules.

Introduction

The chemistry and reactivity of platinum(III) compounds has not yet been explored to the same extent as those of platinum(II) and platinum(IV) species. The majority of platinum(III) complexes have dinuclear structures supported by two[1–3] or four[4–6] bridging ligands. The chelating chain is usually made up of three atoms of the type NCO, NCS, NCN, POP, or OYO (Y = C, S, P), with these three atoms forming a five-membered metallacycle with the two metal centers.[7–9] A few examples of mononuclear platinum(III) species[10] and dinuclear complexes unsupported by covalent bridges have also been reported.[11–13]

Very recently, further interest in dinuclear compounds of platinum(III) has arisen from their potential use as catalysts for the oxidation of olefins.[14–18] This property is fostered by the unusual reactivity of the axial ligands. The axial metal–ligand distances are longer than those found in octahedral platinum(IV) and square-planar platinum(II) complexes but much shorter than distances sometimes found for ligands interacting with platinum(II) species from axial sites.[1]

In spite of the large number of platinum(III) dimers with two or four bridging ligands, very few reports have so far dealt with platinum(III) dimers supported by three covalent bridges. In two NMR investigations, it was shown that species with three acetate bridging ligands can be formed as intermediates in the synthesis of quadruply bridged complexes[19] or as decomposition products of the latter compounds in water,[20] however such species were not isolated or fully characterized.

In this paper, we report the synthesis, NMR characterization, and X-ray structure of the first example of a triply bridged platinum(III) compound with acetamidate ligands, namely $X[Pt_2Cl_4\{N(H)C(CH_3)O\}_3]$ ($X = K^+$ or $AsPh_4^+$).

Results and Discussion

Synthesis and Spectroscopic Characterization

When K_2PtCl_4 and K_2PtCl_6 (1:1 ratio) are allowed to react with a large excess of free amide at high temperature (90 °C) and for a long time (5 h), quadruply bridged dimeric lantern-type complexes are formed. These complexes are insoluble in water and precipitate soon after formation. Full accounts of their synthesis and characterization have already been published.[5,6]

In order to obtain platinum(III) dimers with a smaller number of bridging ligands, we used the same procedure but shortened the reaction time until incipient precipitation of the quadruply bridged species (one instead of five hours). The reaction solution was then filtered and the solvent evaporated to dryness to leave an orange residue. Purification of the crude reaction product was performed by washing with chloroform to remove the excess of acetamide li-

[a] Dipartimento Farmaco-Chimico, Università degli Studi di Bari, Via E. Orabona 4, 70125 Bari, Italy
Fax: +39-080-544-2230
E-mail: natile@farmchim.uniba.it
[b] Dipartimento Geomineralogico, Università degli Studi di Bari, Via E. Orabona 4, 70125 Bari, Italy

gand, extraction with methanol to remove insoluble KCl and trace amounts of unreacted platinum(II) and platinum(IV) species, and finally precipitation with diethyl ether. The orange precipitate was characterized by elemental analysis and IR and NMR spectroscopy, and was found to be the triply bridged species $K[Pt_2Cl_4\{N(H)C(CH_3)O\}_3]$ (**1a**). The corresponding tetraphenylarsonium salt, $(AsPh_4)[Pt_2Cl_4\{N(H)C(CH_3)O\}_3]$ (**1b**), which is soluble in chloroform − **1a** is only soluble in protic solvents such as water and methanol − and precipitates as well-shaped orange crystals from a mixture of chloroform and pentane (1:1, v/v), was also prepared and characterized by elemental analysis, NMR spectroscopy, and X-ray crystallography.

The reaction conditions (90 °C and 1 h reaction time) appear to be critical to maximize the yield of triply bridged species. Longer reaction times result in greater formation of undesired quadruply bridged complexes, while shorter reaction times (0.5 h) leave significant amounts of unreacted platinum(II) and platinum(IV) species. Moreover, if the temperature is lowered the reaction becomes slower and at room temperature does not appear to take place at all.

Since the reaction can lead to formation of several interconverting isomers of the same species (for instance the triply bridged species can be present in three isomeric forms depending upon the relative orientations of the three amidates: HHH, HHT, and HTH), we analyzed the reaction products before and after purification. The latter will be described first.

A solution of **1b** in $CDCl_3$ gives a ^1H NMR spectrum characterized by the presence of two sets of three signals. One set falls in the region of amidic protons (δ = 6.5–5.5 ppm), while the second set falls in the region of aliphatic protons (δ = 2.5–2.0 ppm). The three signals have equal intensities within each set, and the relative intensities of the two sets is 1:3.

The correlations between the two sets of signals were established by a 2D NOESY experiment, which shows a cross peak between the less-shielded amidic proton signal at δ = 6.41 ppm (A) and the less-shielded methyl proton signal at δ = 2.29 ppm (D) and two overlapping cross peaks between the amidic proton signals at δ = 5.75 (B) and 5.73 (C) ppm and the methyl proton signals at δ = 2.03 (F) and 2.05 (E) ppm, respectively (Figure 1).

Three isomers are possible for a dinuclear species with three acetamidate bridging ligands (Figure 2). Two of them, HHH and HTH, have magnetically equivalent acetamidate bridges in *trans* positions, while the third isomer, HHT, has all three acetamidate bridges in different magnetic environments. Since the ^1H NMR spectrum exhibits distinct signals for each of the three acetamidate ligands, we can conclude that the isolated product has an HHT configuration.

The ^{195}Pt NMR spectrum of compound **1b** in $CDCl_3$ reveals the presence of two platinum resonances, one at δ = 241 ppm and the other at δ = –437 ppm. Each resonance is flanked by ^{195}Pt satellites with a $^1J_{Pt,Pt}$ coupling of 6660 Hz (Figure 3).[14,21,22]

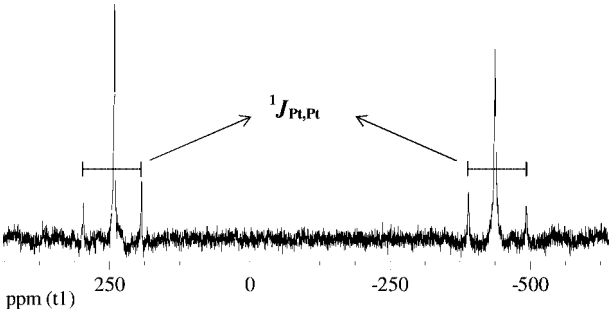

Figure 3. ^{195}Pt NMR spectrum of $(AsPh_4)[Pt_2Cl_4\{N(H)C(CH_3)O\}_3]$ in $CDCl_3$ (4.6×10^{-3} M) at 295 K.

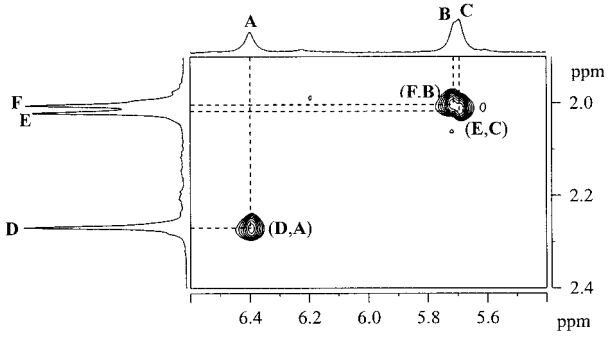

Figure 1. 2D NOESY spectrum of $(AsPh_4)[Pt_2Cl_4\{N(H)C(CH_3)O\}_3]$ in $CDCl_3$ (4.6×10^{-3} M) at 295 K.

On the basis of the established correlations between ^{195}Pt chemical shifts and electronegativities of the donor atoms,[23] the less-shielded signal, at δ = 241 ppm, can be assigned to the Pt atom with Cl_2NO_2 set of donor atoms while the most-shielded signal, at δ = –437 ppm, can be assigned to the Pt atom with Cl_2N_2O set of donor atoms. This assignment is also supported by the broader profile of the peak at δ = –437 ppm as compared to that at δ = 241 ppm. Such a broadening is caused by the N donors, which

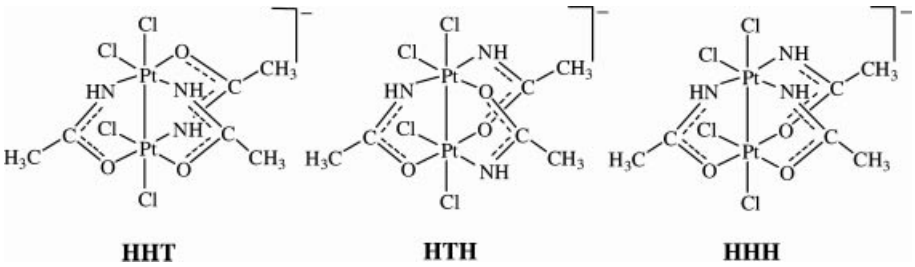

Figure 2. The three possible isomers for the complex $[Pt_2Cl_4\{N(H)C(CH_3)O\}_3]^-$. HH and HT stand for equal (head-to-head) or opposite (head-to-tail) orientation of adjacent amidates, respectively.

number two for the platinum resonating at δ = –437 ppm and only one for the platinum resonating at δ = 241 ppm. It is worth noting that, differently from the present case, where only a broadening of the signals has been observed, the Pt–N couplings are well resolved in some mononuclear complexes with terminal amides.[24]

Compounds **1a** and **1b** in aqueous solution (**1a** is not soluble in $CDCl_3$) give identical ^{195}Pt NMR spectra, with resonances at δ = 220 and –430 ppm indicating that the two compounds contain the same complex anion.

The presence of only one isomer in the purified product indicates that this isomer is the end product of the purification procedure but not necessarily that it is the only product formed in the reaction. For this reason we performed an NMR investigation on the crude reaction product obtained by evaporation of the aqueous reaction solution to dryness. The ^{195}Pt NMR spectrum (due to the presence of a very large excess of free amide the ^1H NMR spectrum is not informative; moreover, water was used as solvent in order to ensure complete dissolution of the raw material) showed the presence of two sets of signals: one corresponding to that of the purified product (signals at δ = 220 and –430 ppm) and the other (signals at δ = 161 and –86 ppm) indicating the presence of a second isomer. The intensity of this second set of signals was initially similar to that of the other isomer (about 0.7 times its intensity). However, on standing in solution at room temperature its intensity decreased and after eight days became negligible (Figure 4). Therefore, we can conclude that two major dinuclear species are initially formed and that with time, under the experimental conditions used for this investigation (water solution of the raw material still containing a large excess of free acetamide), one isomer converts into the other.

It has already been demonstrated that the thermodynamically favored isomer has an HHT configuration, therefore the second isomer observed in the crude reaction product can have either an HTH or an HHH configuration. For the HTH isomer the chemical-shift difference between the two platinum atoms and the peak profiles are expected to be similar to those observed for the HHT isomer since both have similar sets of donor atoms for platinum (Cl_2NO_2 and Cl_2N_2O). In contrast, for the HHH isomer the chemical-shift difference between the two platinum atoms is expected to be greater than for the HHT and HTH isomers due to the greater difference between the sets of donor atoms (Cl_2N_3 and Cl_2O_3). Furthermore, the peak profile is expected to be much broader for $Pt(Cl_2N_3)$ than for $Pt(Cl_2O_3)$. Since the chemical-shift difference between the two platinum atoms and the peak profiles for the second isomer present in the raw material are very similar to those observed for the HHT isomer, we propose that this second isomer has HTH configuration.

X-ray Diffraction Analysis of $(AsPh_4)[Pt_2Cl_4\{N(H)C(CH_3)O\}_3]$

Bond Lengths and Angles

Orange crystals of $\{(AsPh_4)[Pt_2Cl_4\{N(H)C(CH_3)O\}_3]\}_2 \cdot C_5H_{12}$ were obtained by crystallization from $CHCl_3$/pentane (1:1, v/v). The asymmetric unit comprises two independent complex molecules **A** and **B**. The two $[Pt_2Cl_4\{N(H)C(CH_3)O\}_3]^-$ ions are very close to one another, implying the formation of hydrogen bonds between the NH groups of one anion and the O atoms of the second anion. Since the amidate groups in each independent anion are in an HHT arrangement, four different models can be drawn for the pair of independent anions in the asymmetric unit: Z1, Z2, Z3, and Z4 (Scheme 1). The four models converged to R_1 = 0.0375 and wR_2 = 0.0772 for Z1, R_1 = 0.0376 and

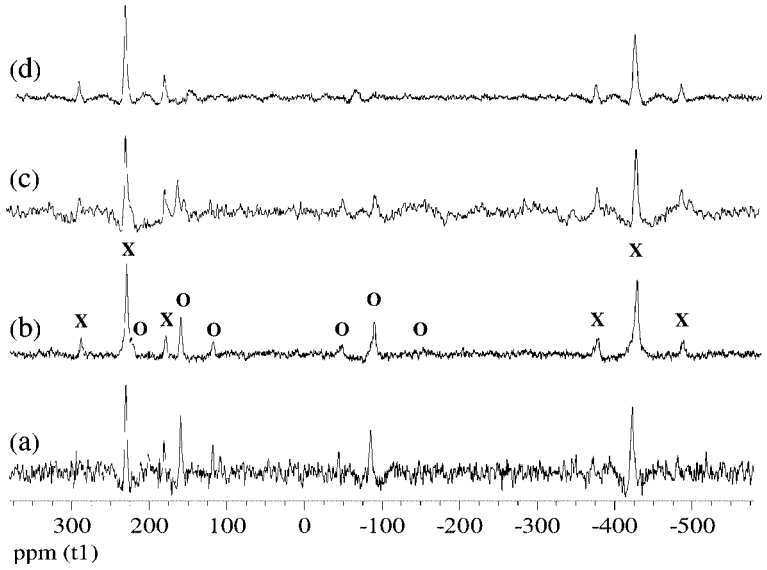

Figure 4. ^{195}Pt NMR spectrum of the crude reaction product dissolved in D_2O and kept at 295 K. The spectra were registered soon after dissolution (a) and after one (b), three (c), and eight (d) days. Resonances of the HHT and HTH isomers are labeled with x and o, respectively.

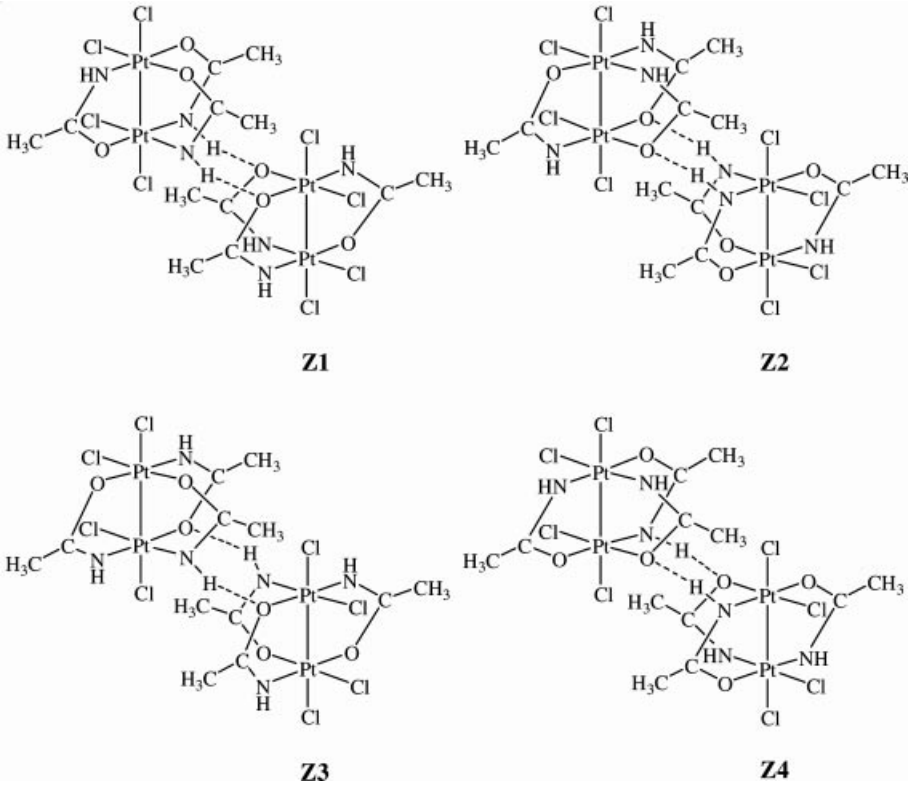

Scheme 1.

wR_2 = 0.0778 for Z2, R_1 = 0.0374 and wR_2 = 0.0766 for Z3, and R_1 = 0.0383 and wR_2 = 0.0811 for Z4. Among these four models, Z3 has the lowest value of wR_2, the best values of thermal parameters for all the N and O atoms of the acetamidate bridging ligands, and the best geometry for the hydrogen bonds between NH and O groups of the two independent anions within the unit cell. On this basis, Z3 was chosen as the correct model. However, clear-cut evidence in favor of Z3 came from analysis of the short contacts between anions of adjacent unit cells. While the Z3 model leads to short (<3.5 Å) N···Cl contacts, indicative of N–H···Cl H-bond interactions, all other models lead to short O···Cl distances, which imply unfavorable electrostatic repulsion between the two electron-rich atoms (see following discussion on intermolecular interactions).

Within a dinuclear complex molecule, each platinum(III) atom has a distorted octahedral geometry with three amidates and a chloride ligand in equatorial positions and a chloride ligand and the second platinum atom in axial positions (Figure 5). Selected bond lengths and angles are reported in Table 1.

The equatorial Pt–Cl [2.27(1)–2.35(1) Å], Pt–N [1.97(2)–2.07(2) Å], and Pt–O distances [2.03(2)–2.08(2) Å] are in the range of those reported for doubly and quadruply bridged dinuclear platinum(III),[5,6,25,26] four-coordinate platinum(II), and six-coordinate platinum(IV) complexes.[11] The axial Pt–Cl distances [2.43(1)–2.47(1) Å] are significantly longer (ca. 0.14 Å) than the equatorial Pt–Cl distances and are comparable to those already reported for axial Pt–Cl distances in dinuclear complexes of platinum(III) (average Pt–Cl distance of 2.44 Å).[5,25–27] The Pt–Pt distances [2.533(2) and 2.527(2) Å] are in between the Pt–Pt distances observed for

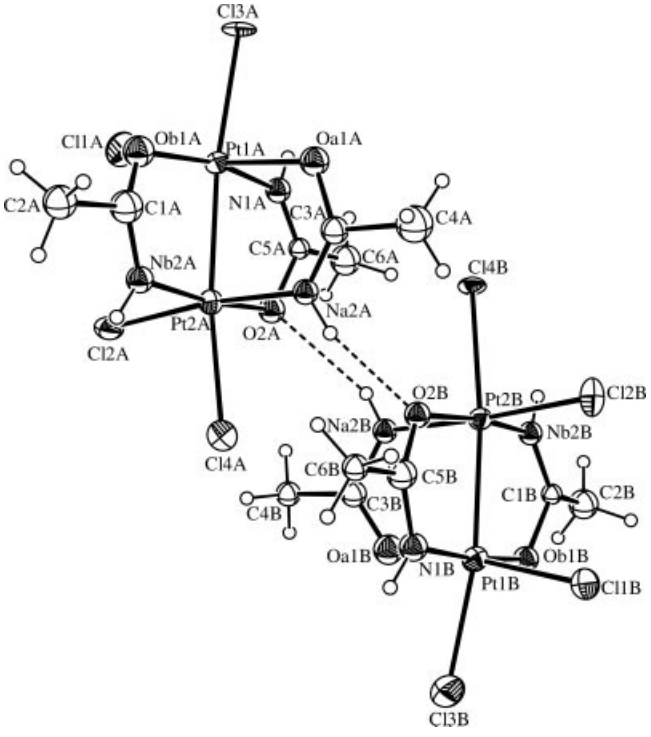

Figure 5. ORTEP view, with labelling scheme, of the two independent $[Pt_2Cl_4\{N(H)C(CH_3)O\}_3]^-$ ions within the unit cell. Ellipsoids enclose 30% probability.

Table 1. Selected bond lengths [Å] and angles [°] for the molecules **A** and **B** of $\{(AsPh_4)[Pt_2Cl_4\{N(H)C(CH_3)O\}_3]\}_2 \cdot C_5H_{12}$.

A		**B**	
Pt(1A)–Pt(2A)	2.527(2)	Pt(1B)–Pt(2B)	2.533(2)
Pt(1A)–N(1A)	2.037(19)	Pt(1B)–N(1B)	1.96(2)
Pt(1A)–O(a1A)	2.058(12)	Pt(1B)–O(a1B)	2.030(13)
Pt(1A)–O(b1A)	2.071(14)	Pt(1B)–O(b1B)	2.051(13)
Pt(1A)–Cl(1A)	2.273(10)	Pt(1B)–Cl(1B)	2.302(10)
Pt(1A)–Cl(3A)	2.455(7)	Pt(1B)–Cl(3B)	2.429(10)
Pt(2A)–N(a2A)	1.970(17)	Pt(2B)–N(b2B)	1.99(2)
Pt(2A)–N(b2A)	2.00(2)	Pt(2B)–N(a2B)	2.074(17)
Pt(2A)–O(2A)	2.083(16)	Pt(2B)–O(2B)	2.040(15)
Pt(2A)–Cl(2A)	2.346(10)	Pt(2B)–Cl(2B)	2.309(10)
Pt(2A)–Cl(4A)	2.448(10)	Pt(2B)–Cl(4B)	2.470(7)
N(1A)–Pt(1A)–O(a1A)	89.0(6)	N(1B)–Pt(1B)–O(a1B)	93.4(6)
O(a1A)–Pt(1A)–O(b1A)	97.5(5)	O(a1B)–Pt(1B)–O(b1B)	80.1(5)
O(b1A)–Pt(1A)–Cl(1A)	86.9(5)	O(b1B)–Pt(1B)–Cl(1B)	93.9(5)
Cl(1A)–Pt(1A)–N(1A)	87.9(6)	Cl(1B)–Pt(1B)–N(1B)	93.1(6)
N(1A)–Pt(1A)–Cl(3A)	93.9(6)	N(1B)–Pt(1B)–Cl(3B)	91.4(7)
O(b1A)–Pt(1A)–Cl(3A)	95.5(4)	O(b1B)–Pt(1B)–Cl(3B)	93.4(5)
O(a1A)–Pt(1A)–Cl(3A)	84.9(4)	O(a1B)–Pt(1B)–Cl(3B)	84.0(5)
Cl(1A)–Pt(1A)–Cl(3A)	87.2(4)	Cl(1B)–Pt(1B)–Cl(3B)	90.5(4)
N(1A)–Pt(1A)–Pt(2A)	84.5(6)	N(1B)–Pt(1B)–Pt(2B)	85.7(6)
O(b1A)–Pt(1A)–Pt(2A)	86.9(4)	O(b1B)–Pt(1B)–Pt(2B)	88.4(4)
O(a1A)–Pt(1A)–Pt(2A)	88.1(4)	O(a1B)–Pt(1B)–Pt(2B)	86.6(4)
Cl(1A)–Pt(1A)–Pt(2A)	99.6(3)	Cl(1B)–Pt(1B)–Pt(2B)	99.2(3)
Cl(3A)–Pt(1A)–Pt(2A)	172.9(2)	Cl(3B)–Pt(1B)–Pt(2B)	170.0(3)
N(a2A)–Pt(2A)–N(b2A)	95.7(7)	N(a2B)–Pt(2B)–N(b2B)	86.6(7)
N(b2A)–Pt(2A)–Cl(2A)	89.1(6)	N(b2B)–Pt(2B)–Cl(2B)	92.9(6)
Cl(2A)–Pt(2A)–O(2A)	87.0(5)	Cl(2B)–Pt(2B)–O(2B)	92.2(5)
O(2A)–Pt(2A)–N(a2A)	89.0(6)	O(2B)–Pt(2B)–N(a2B)	88.7(6)
N(a2A)–Pt(2A)–Cl(4A)	83.8(6)	N(a2B)–Pt(2B)–Cl(4B)	88.3(6)
N(b2A)–Pt(2A)–Cl(4A)	93.1(7)	N(b2B)–Pt(2B)–Cl(4B)	91.1(7)
O(2A)–Pt(2A)–Cl(4A)	95.3(5)	O(2B)–Pt(2B)–Cl(4B)	94.0(5)
Cl(2A)–Pt(2A)–Cl(4A)	90.3(3)	Cl(2B)–Pt(2B)–Cl(4B)	88.2(3)
N(a2A)–Pt(2A)–Pt(1A)	85.6(5)	N(a2B)–Pt(2B)–Pt(1B)	83.9(5)
N(b2A)–Pt(2A)–Pt(1A)	85.1(6)	N(b2B)–Pt(2B)–Pt(1B)	86.5(6)
O(2A)–Pt(2A)–Pt(1A)	87.4(5)	O(2B)–Pt(2B)–Pt(1B)	87.8(4)
Cl(2A)–Pt(2A)–Pt(1A)	100.5(2)	Cl(2B)–Pt(2B)–Pt(1B)	99.6(3)
Cl(4A)–Pt(2A)–Pt(1A)	169.0(3)	Cl(4B)–Pt(2B)–Pt(1B)	171.9(2)

doubly bridged (ca. 2.58 Å)[25–27] and quadruply bridged platinum(III) complexes [2.448(2) Å][5] having bridging amidates and terminal Cl ligands.

The dihedral angles between equatorial planes are 15.3(4)° for molecule **A** and 15.9(4)° for molecule **B**. The bow-like distortion of the Cl3–Pt1–Pt2–Cl4 axis, as indicated by the sum of the deviations from 180° of the angles Cl3–Pt1–Pt2 and Pt1–Pt2–Cl4, is 18.1(4)° for both molecules **A** and **B** and corresponds roughly to the dihedral angle between the equatorial planes. It should be noted that the dihedral angle between the equatorial planes in triply bridged acetamidate species is smaller than in the corresponding doubly bridged species (ca. 20°).[25,26]

Intermolecular Interactions

Compound **1b** crystallizes with one molecule of pentane per asymmetric unit. The molecules of solvent are located in pores of the crystal lattice running along the *a* direction, which appear to be specific for this solvent. For a better understanding of how these pores are formed a detailed description of the crystal packing is given in this section. As already anticipated, two strong H-bonds link the two independent anions (**A** and **B**) within the asymmetric unit. The atoms involved in H-bonding are the nitrogen Na2 and the oxygen O2 [Na2A···O2B = 2.92(2), (Na2A)H···O2B = 2.09(1) Å, Na2A–H···O2B = 162(1)°; Na2B···O2A = 3.09(2), (Na2B)H···O2A = 2.36(2) Å, Na2B–H···O2A = 142(1)°].

Anions **A** and **B** of one cell are hydrogen-bonded with anions of adjacent cells. These H-bonds involve the Cl4 and Nb2 atoms of anion **A** of one cell and the Nb2 and Cl4 atoms of anion **B** of the adjacent cell [Nb2A···Cl4B(x + 1, +y, +z) = 3.49(2), (Nb2A)H···Cl4B(x + 1, +y, +z) = 2.664(7) Å, Nb2A–H···Cl4B(x + 1, +y, +z) = 162(1)°; Nb2B···Cl4A(x – 1, +y, +z) = 3.46(2), (Nb2B)H···Cl4A(x – 1, +y, +z) = 2.615(9) Å, Nb2B–H···Cl4A(x – 1, +y, +z) = 170(1)°].

As already anticipated, all the models other than Z3 reported in Scheme 1 (Z1, Z2, and Z4) would result in very short O···Cl nonbonding distances between contiguous **A** and **B** anions of adjacent cells. The resulting O···Cl distances (ca. 3.46 Å) would be very close to the sum of the van der Waals radii for oxygen and chlorine atoms and would lead to unfavorable electrostatic repulsion between

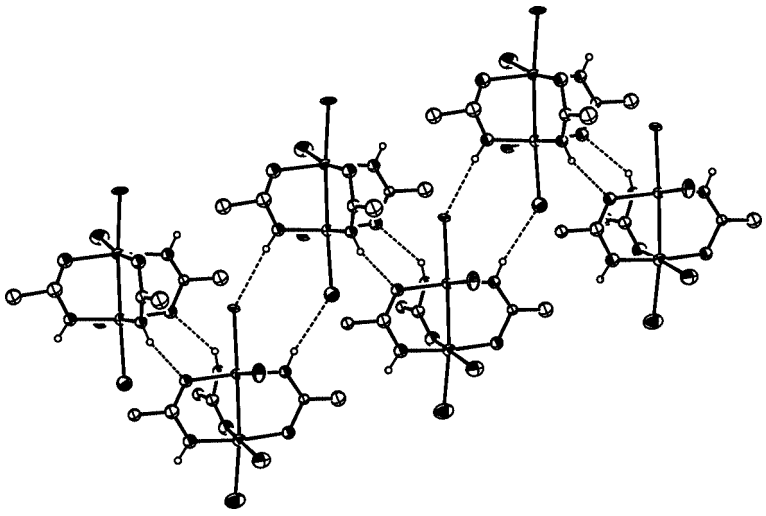

Figure 6. View of the hydrogen-bonding network.

the two electron-rich atoms. This observation gives strong support to the choice of model Z3 for describing the positioning of the two anions within the unit cell.

The N–H···O hydrogen bonds linking the **A** and **B** molecules within the same cell and the N–H···Cl bonds linking the **A** molecule of one cell with the **B** molecule of the adjacent cell make a chain of $[Pt_2Cl_4\{N(H)C(CH_3)O\}_3]^-$ anions extending along the *a* axis (Figure 6).

The tetraphenylarsonium cations are located between the chains of anions extending along the *a* direction, which results in columns running parallel to the chains of anions. There are no direct interactions between these cations, however there are H-bonds between the Cl atoms of the chains of anions and the H atoms of the cations [Cl1A···C20A = 3.46(2), Cl1A···H(C20A) = 2.72(1) Å, Cl1A···H–C20A = 137(1)°; Cl1A···C29B($x-1, y-1, z-1$) = 3.77(2), Cl1A···H(C29B)($x-1, y-1, z-1$) = 3.00(1) Å, Cl1A···H–C29B($x-1, y-1, z-1$) = 141(1)°; Cl2A···C11A = 3.55(2), Cl2A···H(C11A) = 2.79(1) Å, Cl2A···H–C11A = 140(1)°; Cl2A···C27A($x+1, y, z$) = 3.60(2), Cl2A···H(C27A)($x+1, y, z$) = 2.72(1) Å, Cl2A···H–C27A($x+1, y, z$) = 158(1)°; Cl3A···C30B($x-1, y-1, z-1$) = 3.46(2), Cl3A···H(C30B)($x-1, y-1, z-1$) = 2.77(1) Å, Cl3A···H–C30B($x-1, y-1, z-1$) = 132(1)°; Cl4A···C15B($x, y, z-1$) = 3.63(2), Cl4A···H(C15B)($x, y, z-1$) = 2.73(1) Å, Cl4A···H–C15B($x, y, z-1$) = 162(1)°; Cl1B···C8B = 3.55(2), Cl1B···H(C8B) = 2.72(1) Å, Cl1B···H–C8B = 149(1)°; Cl2B···C15A($x, y, z+1$) = 3.56(2), Cl2B···H(C15A)($x, y, z+1$) = 2.70(1) Å, Cl2B···H–C15A($x, y, z+1$) = 153(1)°; Cl3B···C30A($x+1, y+1, z+1$) = 3.67(2), Cl3B···H(C30A)($x+1, y+1, z+1$) = 2.99(1) Å, Cl3B···H–C30A($x+1, y+1, z+1$) = 132(1)°; Cl4B···C27B($x-1, y, z$) = 3.80(2), Cl4B···H(C27B)($x-1, y, z$) = 2.99(1) Å, Cl4B···H–C27B($x-1, y, z$) = 146(1)°; Cl4B···C14A($x, y, z+1$) = 3.67(2), Cl4B···H(C14A)($x, y, z+1$) = 2.95(1) Å, Cl4B···H–C14A($x, y, z+1$) = 135(1)°]. The packing of the chains of anions and columns of cations extending along the *a* direction leaves some channels, which also extend along the *a* direction; the pentane molecules of crystallization are located in these channels (Figure 7).

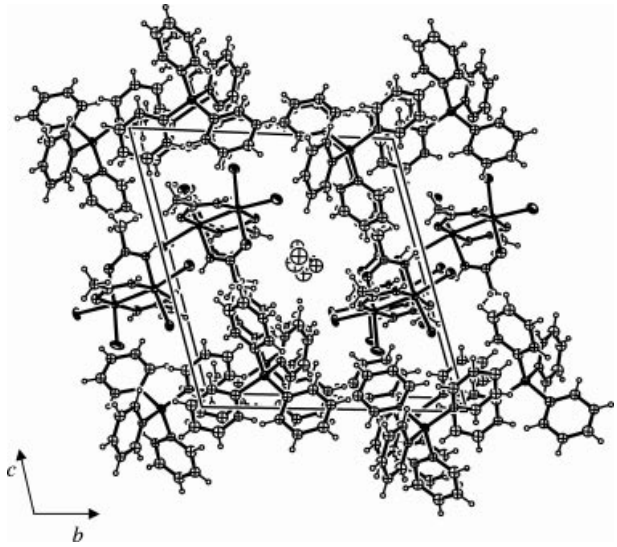

Figure 7. Crystal packing of $\{(AsPh_4)[Pt_2Cl_4\{N(H)C(CH_3)O\}_3]\}_2 \cdot C_5H_{12}$, showing the location of the solvent molecules in the pores of the crystal lattice.

Conclusions

Dimeric platinum(III) complexes supported by three covalent bridges between the two metal centers have generally been considered as transient species in the reaction leading to quadruply bridged species starting from a 1:1 mixture of Pt^{II} and Pt^{IV} chloro species and excess bridging ligand. We have proven that, by reducing the reaction time, the triply bridged compound can become the major reaction product.

Due to the asymmetry of the acetamide ligand, three isomers can be formed (HHH, HHT, and HTH), although only two major species were found in the crude reaction product: HHT and HTH. Moreover, the HTH species is

thermodynamically less stable and slowly (half life of about two days at room temperature) isomerizes into the HHT form. A possible explanation for the observed preference is the more homogeneous sets of donor atoms for the two platinum atoms provided by the HHT and HTH isomers (Cl_2N_2O and Cl_2NO_2) as compared to the HHH isomer (Cl_2N_3 and Cl_2O_3). The HHT isomer is favored over the HTH isomer by a statistical factor of two. It should be noted that the greater stability of the HHT isomer is also in agreement with the configurations found in the quadruply bridged dimers prepared by a similar reaction procedure.[5] The preferred configurations were usually found to be HHTH and HHTT. These two configurations can both be generated from the triply bridged HHT species by addition of a fourth bridge in an H or T orientation. In contrast, the HTH isomer can generate, upon the addition of a fourth bridge, only one observed configuration (HTHH) and a second, never observed, configuration (HTHT).

The crystal structure of the more stable and less symmetric HHT isomer is made up of chains of $[Pt_2Cl_4\{N(H)C(CH_3)O\}_3]^-$ ions running along the *a* direction and columns of tetraphenylarsonium cations also running along the *a* direction. A curious aspect of the crystal packing is the presence of one-dimensional pore channels filled with disordered pentane molecules. The dimension of the pore is probably such that only molecules of *n*-pentane can be accommodated, leaving out completely the molecules of chloroform which, in principle, should give stronger interactions (H bonds) with the aromatic protons on the surface of the pores.

Experimental Section

Physical Measurements: Elemental analyses were obtained with an Elementar Analyser mod. 1106 Carlo Erba instrument. ^1H and ^{195}Pt NMR spectra were recorded with a Bruker Avance DPX 300 WB spectrometer. ^1H chemical shifts are referenced to TMS and ^{195}Pt chemical shifts to K_2PtCl_4 (1 M in water, δ = –1614 ppm).

Preparation of $K[Pt_2Cl_4\{N(H)C(CH_3)O\}_3]$ (1a): K_2PtCl_4 (500 mg, 1.2 mmol) and K_2PtCl_6 (585 mg, 1.2 mmol) were dissolved in water (25 mL) and treated with an excess of acetamide (2.8 g, 48 mmol). The reaction mixture was stirred for 1 h at 90 °C. The resulting red solution was cooled to room temperature and then taken to dryness under reduced pressure. The orange solid residue was washed several times with small portions of chloroform in order to remove the excess of acetamide and then extracted with methanol, which solubilizes only the desired compound (**1a**) while leaving KCl and unreacted K_2PtCl_6 and K_2PtCl_4 as insoluble residue. Orange microcrystals of $K[Pt_2Cl_4\{N(H)C(CH_3)O\}_3]$ precipitated from the methanolic solution upon addition of diethyl ether. Yield: 45% (400 mg). $K[Pt_2Cl_4\{N(H)C(CH_3)O\}_3]\cdot 2H_2O$, $C_6H_{16}Cl_4KN_3O_5Pt_2$ (780.9): calcd. C 9.21, H 2.05, N 5.38; found C 8.83, H 1.83, N 5.54. ^{195}Pt NMR (64.3 MHz, D_2O, 22 °C): δ = –430 ($PtCl_2N_2O$) and 220 ($PtCl_2NO_2$) ppm ($^1J_{Pt,Pt}$ = 7020 Hz).

Preparation of $(AsPh_4)[Pt_2Cl_4\{N(H)C(CH_3)O\}_3]$ (1b): $K[Pt_2Cl_4\{N(H)C(CH_3)O\}_3]$ (400 mg, 0.54 mmol) and $AsPh_4Cl$ (339 mg, 0.81 mmol) were dissolved in chloroform (70 mL) and stirred for a few minutes. The white precipitate of KCl was removed while the filtered mother liquor was concentrated to a smaller volume (10 mL) and then layered with pentane (10 mL). Under these conditions, orange crystals of the desired product $(AsPh_4)[Pt_2Cl_4\{N(H)C(CH_3)O\}_3]$ separated from solution. Yield: 23% (135 mg). $\{(AsPh_4)[Pt_2Cl_4\{N(H)C(CH_3)O\}_3]\}_2\cdot C_5H_{12}$, $C_{65}H_{76}Cl_8N_6O_6Pt_4As_2$ (2249.4): calcd. C 34.69, H 3.40, N 3.73; found C 34.78, H 3.27, N 3.50. ^1H NMR (300 MHz, $CDCl_3$, 22 °C): δ = 2.03 (s, 3 H, CH_3), 2.05 (s, 3 H, CH_3), 2.29 (s, 3 H, CH_3), 5.73 (s, 1 H, NH), 5.75 (s, 1 H, NH), 6.41 (s, 1 H, NH) ppm. ^{195}Pt NMR (64.3 MHz, $CDCl_3$, 22 °C): δ = –437 ($PtCl_2N_2O$) and 241 ($PtCl_2NO_2$) ppm ($^1J_{Pt,Pt}$ = 6660 Hz).

X-ray Crystal Structure Determination of $\{(AsPh_4)[Pt_2Cl_4\{N(H)C(CH_3)O\}_3]\}_2\cdot C_5H_{12}$: Compound **1b**, which crystallizes from $CHCl_3$/pentane with half a molecule of pentane per molecule of compound, was investigated by X-ray diffraction analysis. X-ray data were collected on a BrukerAXS X8 APEX CCD system equipped with a four-circle Kappa goniometer and a 4 K CCD detector (Mo-K_α radiation). A Miracol fiber optics capillary collimator (0.3 mm) was used to enhance the intensity of the Mo-K_α radiation and to reduce X-ray beam divergence. The diameter of the active imaging area was 90 mm and the data were collected at a resolution of 512 × 512 pixels. The crystal-to-detector distance was 40 mm. The SAINT-IRIX package was employed for data reduction and unit-cell refinement.[28]

A total of 53118 reflections (Θ_{max} = 25.00°) were indexed, integrated, and corrected for Lorentz, polarization, and absorption effects using the program SADABS.[29] The number of independent reflections was 12139. The unit-cell dimensions were calculated from all reflections. The structure was solved by direct methods technique in the *P*1 space group. A pseudo center of inversion is present between the two dinuclear independent molecules **A** and **B**, which is reminiscent of a virtual $P\bar{1}$ space group, although attempts to refine in this group were unsuccessful.

Table 2. Crystal data and structure-refinement parameters for $\{(AsPh_4)[Pt_2Cl_4\{N(H)C(CH_3)O\}_3]\}_2\cdot C_5H_{12}$.

Empirical formula	$C_{65}H_{76}As_2Cl_8N_6O_6Pt_4$
Formula mass	2315.12
Temperature	293(2) K
Wavelength	0.71073 Å
Crystal system	triclinic
Space group	*P*1
Unit-cell dimensions	*a* = 8.6244(3) Å α = 104.322(2)°
	b = 14.6244(5) Å β = 97.420(2)°
	c = 15.3213(5) Å γ = 105.320(2)°
V	1766.28(10) Å^3
Z	1 (A + B)
$D_{calcd.}$	2.177 g cm^{-3}
μ	9.190 mm^{-1}
F(000)	1102
Crystal size	0.036 × 0.224 × 0.010 mm
θ range	1.40–25.00°
Index ranges	$-10 \le h \le 10$
	$-17 \le k \le 17$
	$-18 \le l \le 18$
Reflections collected	53153
Independent reflections	12146 [*R*(int) = 0.0721]
Absorption correction	SADABS (Sheldrick, 1996)
Refinement method	Full-matrix least-squares on F^2
Data/restraints/parameters	12146/3/349
Goodness-of-fit on F^2	1.012
Final *R* indices [$I > 2\sigma(I)$]	R_1 = 0.0374, wR_2 = 0.0766
R indices (all data)	R_1 = 0.0676, wR_2 = 0.0873
Absolute structure parameter	0.00(1)
Largest diff. peak and hole	0.966 and –0.659 e Å^{-3}

The model was refined by full-matrix least-square methods. Only the Pt, Cl, and As atoms were refined anisotropically; the remaining atoms needed isotropic treatment in order to maintain satisfactory thermal displacement parameters. Furthermore, the phenyl groups were treated as rigid, idealized hexagons. Hydrogen atoms were placed at calculated positions and refined given isotropic parameters equivalent to 1.2-times (for phenyl groups) or 1.5-times (for methyl groups) those of the atom to which they are attached.

The pentane solvent molecule of crystallization was disordered. The final difference-Fourier map showed electron density peaks (up to 0.966 e $Å^{-3}$) lying near the Pt atoms. All calculations and molecular graphics were carried out using the SIR2002,[30] SHELXL97,[31] PARST97,[32] WinGX,[33] or ORTEP-3 for Windows packages.[34] The crystallographic data are listed in Table 2.

CCDC-288044 contains the supplementary crystallographic data for this paper. These data can be obtained free of charge from The Cambridge Crystallographic Data Center via www.ccdc.cam.ac.uk/data_request/cif.

Acknowledgments

The authors thank the Università degli Studi di Bari (ex. 60% funds), the Italian "Ministero dell'Istruzione, Università e Ricerca (MIUR)" (PRIN 2004 no. 2004059078_006), and the EC (COST Chemistry projects D20/0001/2000 and D20/0003/01) for support.

[1] K. Matsumoto, K. Sakai, *Adv. Inorg. Chem.* **1999**, *49*, 375–427.
[2] W. Chen, K. Matsumoto, *Inorg. Chim. Acta* **2003**, *342*, 88–96.
[3] B. Lippert, *Coord. Chem. Rev.* **1999**, *181*, 263–295.
[4] T. N. Fedotova, L. K. Minacheva, G. N. Kuznetsova, V. G. Sakharova, M. I. Gel'fman, I. B. Baranovskii, *Russ. J. Inorg. Chem.* **1997**, *42*, 1838–1846.
[5] A. Dolmella, F. P. Intini, C. Pacifico, G. Padovano, G. Natile, *Polyhedron* **2002**, *21*, 275–280.
[6] G. Bandoli, A. Dolmella, F. P. Intini, C. Pacifico, G. Natile, *Inorg. Chim. Acta* **2003**, *346*, 143–150.
[7] G. Natile, F. P. Intini, C. Pacifico, in *Cisplatin*: *Chemistry and Biochemistry of a Leading Anticancer Drug* (Ed.: B. Lippert), Verlag Helvetica Chimica Acta Zürich, Switzerland, and Wiley-VCH, Weinheim, Germany, **1999**; p. 429–453.
[8] K. Umakoshi, Y. Sasaki, *Adv. Inorg. Chem.* **1993**, *40*, 187–239.
[9] G. Kampf, M. Willermann, E. Zangrando, L. Randaccio, B. Lippert, *Chem. Commun.* **2001**, 747–748.
[10] a) T. V. O'Halloran, S. J. Lippard, *Isr. J. Chem.* **1985**, *25*, 130–137; b) O. Renn, A. Albinati, B. Lippert, *Angew. Chem. Int. Ed. Engl.* **1990**, *29*, 84–85; c) M. Kurmoo, R. J. Clark, *Inorg. Chem.* **1985**, *24*, 4420–4425; d) C. S. Glennon, T. D. Hand, A. G. Sykes, *J. Chem. Soc., Dalton Trans.* **1980**, 19–23; e) K. K. S. Gupta, P. K. Sen, S. S. Gupta, *Inorg. Chem.* **1977**, *16*, 1396–1399; f) J. Halpern, M. Pribanic, *J. Am. Chem. Soc.* **1968**, *90*, 5942–5943; g) C. V. Chan, L. K. Cheng, C.-M. Che, *Coord. Chem. Rev.* **1994**, *132*, 87–97; h) J. Forniés, B. Menjon, R. M. Sanz-Carrillo, M. Tomas, N. G. Connelly, J. G. Crossley, A. G. Orpen, *J. Am. Chem. Soc.* **1995**, *117*, 4295–4304.
[11] R. Cini, F. P. Fanizzi, F. P. Intini, G. Natile, *J. Am. Chem. Soc.* **1991**, *113*, 7805–7806.
[12] R. Cini, F. P. Fanizzi, F. P. Intini, L. Maresca, G. Natile, *J. Am. Chem. Soc.* **1993**, *115*, 5123–5131.
[13] G. Bandoli, P. A. Caputo, F. P. Intini, M. F. Sivo, G. Natile, *J. Am. Chem. Soc.* **1997**, *119*, 10370–10376.
[14] K. Matsumoto, J. Matsunami, K. Mizuno, H. Uemura, *J. Am. Chem. Soc.* **1996**, *118*, 8959–8960.
[15] K. Matsumoto, Y. Nagai, J. Matsunami, K. Mizuno, T. Abe, R. Somazawa, J. Kinoshita, H. Shimura, *J. Am. Chem. Soc.* **1998**, *120*, 2900–2907.
[16] Y. Lin, S. Takeda, K. Matsumoto, *Organometallics* **1999**, *18*, 4897–4899.
[17] N. Saeki, N. Nakamura, T. Ishibashi, M. Arime, H. Sekiya, K. Ishihara, K. Matsumoto, *J. Am. Chem. Soc.* **2003**, *125*, 3605–3616.
[18] M. Ochiai, Y. Lin, J. Yamada, H. Misawa, S. Arai, K. Matsumoto, *J. Am. Chem. Soc.* **2004**, *126*, 2536–2545.
[19] T. G. Appleton, K. A. Byriel, J. M. Garrett, J. R. Hall, C. H. L. Kennard, M. T. Mathieson, R. Stranger, *Inorg. Chem.* **1995**, *34*, 5646–5655.
[20] T. G. Appleton, K. A. Byriel, J. R. Hall, C. H. L. Kennard, M. T. Mathieson, *J. Am. Chem. Soc.* **1992**, *114*, 7305–7307.
[21] T. G. Appleton, J. R. Hall, D. W. Neale, S. F. Ralph, *Inorg. Chim. Acta* **1983**, *77*, L149–L151.
[22] T. G. Appleton, J. R. Hall, D. W. Neale, *Inorg. Chim. Acta* **1985**, *104*, 19–31.
[23] P. S. Pregosin, "Platinum NMR Spectroscopy", *Annu. Rep. NMR Spectrosc.* **1986**, *17*, 285–349.
[24] R. Cini, F. P. Fanizzi, F. P. Intini, G. Natile, C. Pacifico, *Inorg. Chim. Acta* **1996**, *251*, 111–118.
[25] B. Lippert, H. Scholhorn, U. Thewalt, *Inorg. Chem.* **1986**, *25*, 407–408.
[26] L. S. Hollis, M. M. Roberts, S. J. Lippard, *Inorg. Chem.* **1983**, *22*, 3637–3644.
[27] K. Sakai, Y. Tanaka, Y. Tsuchiya, K. Hirata, T. Tsubomura, S. Iijima, A. Bhattacharjee, *J. Am. Chem. Soc.* **1998**, *120*, 8366–8379.
[28] Bruker: SAINT-IRIX. Bruker AXS Inc., Madison, Wisconsin, USA, **2003**.
[29] G. M. Sheldrick, *SADABS, Program for Empirical Absorption Correction of Area Detector Data*, University of Göttingen, Germany, **1996**.
[30] Sir2002: M. C. Burla, M. Camalli, B. Carrozzini, G. L. Cascarano, C. Giacovazzo, G. Polidori, R. Spagna, *J. Appl. Crystallogr.* **2003**, *36*, 1103.
[31] *Programs for Crystal Structure Analysis (release 97-2)*, G. M. Sheldrick, Institut für Anorganische Chemie der Universität, Tammanstrasse 4, 37077 Göttingen, Germany, **1998**.
[32] a) M. Nardelli, *Comput. Chem.* **1983**, *7*, 95–97; b) M. Nardelli, *J. Appl. Crystallogr.* **1995**, *28*, 659.
[33] L. J. Farrugia, *J. Appl. Crystallogr.* **1999**, *32*, 837–838.
[34] L. J. Farrugia, *J. Appl. Crystallogr.* **1997**, *30*, 565.

Received: October 27, 2005
Published Online: March 1, 2006

